Inorg. Chem. **2003**, *42*, 4417–4424

$Cl_3V(\mu\text{-}S(CH_3)_2)_3VCl_3^{2-}$: A First-Row, Face-Shared Bioctahedral Complex with Multiple Metal–Metal Bonding

Simon Petrie and Robert Stranger*

Department of Chemistry, the Faculties, the Australian National University, Canberra ACT 0200, Australia

Received December 16, 2002

Density functional theory calculations have been used to investigate the structure and bonding of the d^3d^3 bioctahedral complexes $X_3V(\mu\text{-}S(CH_3)_2)_3VX_3^{2-}$ ($X = F^-$, Cl^-, OH^-, SH^-, NH_2^-). According to geometry optimizations using the broken-symmetry approach and the VWN+B-LYP combination of density functionals, the halide-terminated complexes have a V–V bond order of approximately 2, while complexes featuring OH^-, SH^-, or NH_2^- as terminal ligands exhibit full triple bonding between the vanadium atoms. The tendency toward triple bonding in the latter complexes is consistent with an increased covalency of the vanadium–ligand bonds, and the influence of bond covalency is apparent also in the tendency for V–V bond elongation in the complexes with OH^- and NH_2^- terminal ligands. Detailed examination of the composition of molecular orbitals in all of the thioether-bridged V^{II} complexes substantiates the conclusion that the strong antiferromagnetic coupling which we have determined for these complexes ($-J > 250$ cm^{-1}) is due to direct bonding between metal atoms rather than superexchange through the bridging ligands. As such, these V^{II} complexes comprise the first apparent examples of multiple metal–metal bonding in first-transition-row, face-shared dinuclear complexes and are therefore of considerable structural and synthetic interest.

Introduction

Face-shared d^3d^3 bioctahedral complexes, as typified by $Cr_2Cl_9^{3-}$, exhibit considerable structural variety. This is particularly true of their intermetallic interactions, which range from essentially localized structures (such as $Cr_2Cl_9^{3-}$ itself) featuring long metal−metal separations [e.g., r(Cr−Cr) ∼ 3.10 Å][1−5] to strongly bonded complexes [e.g., $W_2Cl_9^{3-}$, r(W−W) ∼ 2.45 Å][6−8] with short, formally triple-bonded, metal−metal distances. The face-shared bioctahedral complexes have received considerable attention from computational chemists,[9−22] who have sought to identify the factors influencing adoption either of a weakly coupled, essentially nonbonded interaction between metal atoms or of a strong multiple metal−metal bond. While such studies have shown that the interplay between weak coupling and strong metal−metal bonding depends on several factors, it is also apparent that perhaps the most crucial parameter is the radial extent of the valence d orbitals on the respective metals. Hence, the general tendency is for complexes featuring third-row transition metals to exhibit multiple bonding, while first-row complexes are much more weakly coupled and second-row species adopt an intermediate configuration.

* Author to whom correspondence should be addressed. E-mail: rob.stranger@anu.edu.au.

(1) Wessel, G. J.; Ijdo, D. J. W. *Acta Crystallogr.* **1957**, *10*, 466.
(2) Cotton, F. A. *Rev. Pure Appl. Chem.* **1967**, *17*, 25.
(3) Grey, I. E.; Smith, P. W. *Aust. J. Chem.* **1971**, *24*, 73.
(4) Barry, K. R.; Maxwell, K. J.; Siddiqui, K. A.; Stevens, K. W. H. *J. Phys. C* **1981**, *14*, 1281.
(5) Leuenberger, B.; Guedel, H. U. *Inorg. Chem.* **1986**, *25*, 181.
(6) Watson, W. H., Jr.; Waser, J. *Acta Crystallogr.* **1958**, *11*, 689.
(7) Dunbar, K. R.; Pence, L. E. *Acta Crystallogr.* **1991**, *C47*, 23.
(8) Stranger, R.; Grey, I. E.; Madsen, I. C.; Smith, P. W. *J. Solid State Chem.* **1987**, *69*, 162.
(9) Jacobsen, H.; Kraatz, H. B.; Ziegler, T.; Boorman, P. M. *J. Am. Chem. Soc.* **1992**, *114*, 7851.
(10) Medley, G. A.; Stranger, R. *Inorg. Chem.* **1994**, *33*, 3976.
(11) Lovell, T.; McGrady, J. E.; Stranger, R.; Macgregor, S. A. *Inorg. Chem.* **1996**, *35*, 3079.
(12) McGrady, J. E.; Lovell, T.; Stranger, R. *Inorg. Chem.* **1997**, *36*, 3242.
(13) McGrady, J. E.; Stranger, R.; Lovell, T. *J. Phys. Chem. A* **1997**, *101*, 6265.
(14) McGrady, J. E.; Stranger, R.; Lovell, T. *Inorg. Chem.* **1998**, *37*, 3802.
(15) Stranger, R.; McGrady, J. E.; Lovell, T. *Inorg. Chem.* **1998**, *37*, 6795.
(16) Delfs, C. D.; Stranger, R. *Inorg. Chem.* **2000**, *39*, 491.
(17) Lovell, T.; Stranger, R.; McGrady, J. E. *Inorg. Chem.* **2001**, *40*, 39.
(18) Stranger, R.; Turner, A.; Delfs, C. D. *Inorg. Chem.* **2001**, *40*, 4093.
(19) Petrie, S.; Stranger, R. *Inorg. Chem.* **2002**, *41*, 2341.
(20) Petrie, S.; Stranger, R. *Polyhedron* **2002**, *21*, 1163.
(21) Stranger, R.; Petrie, S. *Dalton Trans.* **2002**, 3630.
(22) Petrie, S.; Stranger, R. *Inorg. Chem.* **2002**, *41*, 6291.

10.1021/ic026276k CCC: $25.00
Published on Web 06/11/2003

Niemann et al.[23] have summarized some of the key structural and magnetic parameters for a set of 16 first-row, face-shared bioctahedra. Notably, the eight complexes in their survey with metal−metal separations r(M−M) < 2.7 Å all feature μ-oxo, μ-hydroxo, or μ-alkoxo bridges, while the complexes with r(M−M) > 2.7 Å are exclusively μ-halide-bridged. The three largest-magnitude values of the spin-exchange coupling constant, J, reported in the survey of Niemann et al.[23] are −340, −256, and −125 cm^{-1} for complexes featuring respectively three, two, and one μ-oxo bridges. Excluding μ-oxo-bridged complexes, for which superexchange (rather than direct metal−metal bonding) has been shown to dominate the magnetic coupling in both edge-shared[24,25] and face-shared[16] dinuclear complexes, none of the Niemann et al. survey's[23] complexes have a measured J value of greater magnitude than −100 cm^{-1}. In the intervening decade, the synthesis of several novel first-row, face-shared d^3d^3 dinuclear complexes[26−32] has seen a substantial proliferation in the variety of bridging ligands employed in Cr(III) and Mn(IV) complexes but has not provided any new examples of strongly antiferromagnetic, face-sharing, first-row complexes.

While several different bridging ligands have been exploited in studies on first-row binuclear complexes, we are unaware of any reported first-row, face-sharing dimers featuring thioether bridges. Such complexes are of interest for at least two reasons. First, there are several extant Nb(II) and Ta(II) face-sharing complexes of tetrahydrothiofuran (tht, C_4H_8S),[33−35] all of which are known to possess short and strong (nominally triple) M−M bonds. Second, a density functional theory (DFT) study by Ziegler and coworkers[9] has noted that substitution by thioethers of chloride bridges in Mo(III) dinuclear complexes leads to a considerable contraction in the Mo−Mo separation. The apparent ability of thioethers to stabilize short M−M bonds in these second- and third-row dinuclear complexes, as shown also by our own previous DFT calculations[22] on models of the known Nb(II) and Ta(II) examples, led us to wonder whether such stabilization might also occur in first-row complexes, and this query forms the basis of the present work.

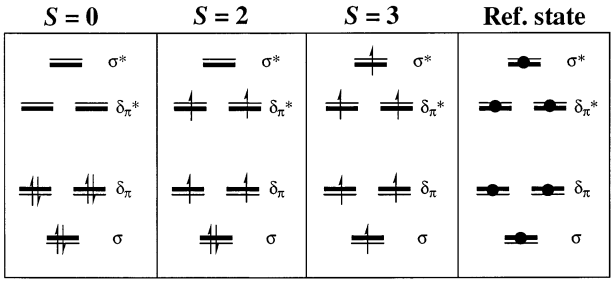

Figure 1. Representation of t_{2g}-derived orbital occupancy for the $S = 0$, $S = 2$, and $S = 3$ associated states, and for the reference state, for a face-shared d^3d^3 dimer $X_3M(\mu\text{-}Y)_3MX_3^{n-}$.

Computational Details

All calculations described in this work were performed on Linux-based Pentium IV 1.7−2.0 GHz computers using the Amsterdam Density Functional (ADF) program, version ADF2002,[36] developed by Baerends et al.[37,38] Each calculation used one of three combinations of functionals: (i) the local density approximation (LDA) to the exchange potential[39] and the local correlation potential of Vosko, Wilk, and Nusair (VWN);[40] (ii) the VWN local correlation potential, the Becke nonlocal exchange potential,[41] and the Lee−Yang−Parr correlation potential[42] in a combination identified as VWN+B-LYP; or (iii) the local (LDA) exchange potential, Becke nonlocal exchange, and Lee−Yang−Parr nonlocal correlation. The latter combination of functionals is widely used by many researchers and is generally abbreviated as B-LYP. The triple-ζ plus polarization basis sets, featuring Slater-type orbitals, were used for all atoms. Electrons in orbitals up to and including 1s {C, N, O, F} or 2p {S, Cl, V} were treated in accordance with the frozen-core approximation. Optimized geometries were obtained using the gradient algorithm of Versluis and Ziegler.[43] Full-symmetry calculations for the $S = 0$, $S = 2$, and $S = 3$ associated states (see Figure 1), and "reference state" calculations of the type described previously,[12] were performed in a spin-unrestricted manner using D_{3h} symmetry. Broken-symmetry (BS) calculations for the $M_S = 0$ state (employing an asymmetry in the initial spin densities upon the two metal atoms)[44] were executed in C_{3v} symmetry. Potential energy curves for the BS state, and in some instances for the associated states, were obtained by optimization of all other structural parameters for the dimers along a series of fixed metal−metal separations. While in most calculations the default geometry optimization convergence

(23) Niemann, A.; Bossek, U.; Wieghardt, K.; Butzlaff, C.; Trautwein, A. X.; Nuber, B. *Angew. Chem., Int. Ed. Engl.* **1992**, *31*, 311.
(24) McGrady, J. E.; Stranger, R. *J. Am. Chem. Soc.* **1997**, *119*, 8512.
(25) McGrady, J. E.; Stranger, R. *Inorg. Chem.* **1999**, *38*, 550.
(26) Glerup, J.; Larsen, S.; Weihe, H. *Acta Chem. Scand.* **1993**, *47*, 1154.
(27) Hage, R.; Krijnen, B.; Warnaar, J. B.; Hartl, F.; Stufkens, D. J.; Snoeck, T. L. *Inorg. Chem.* **1995**, *34*, 4973.
(28) Lueken, H.; Schilder, H.; Jacobs, H.; Zachwieja, U. *Z. Anorg. Allg. Chem.* **1995**, *621*, 959.
(29) Maragh, P. T.; Dasgupta, T. P.; Williams, D. J. *J. Chem. Soc., Dalton Trans.* **1995**, 2843.
(30) Fujihara, T.; Fuyuhiro, A.; Kaizaki, S. *Inorg. Chim. Acta* **1998**, *278*, 15.
(31) Schenker, R.; Weihe, H.; Guedel, H. U.; Kersting, B. *Inorg. Chem.* **2001**, *40*, 3355.
(32) Schenker, R.; Heer, S.; Guedel, H. U.; Weihe, H. *Inorg. Chem.* **2001**, *40*, 1482.
(33) Cotton, F. A.; Diebold, M. P.; Roth, W. J. *J. Am. Chem. Soc.* **1987**, *109*, 5506.
(34) Babainkibala, E.; Cotton, F. A.; Shang, M. *Acta Crystallogr. C* **1991**, *47*, 1617.
(35) Cotton, F. A.; Shang, M. *Inorg. Chim. Acta* **1994**, *227*, 191.
(36) Baerends, E. J.; Autschbach, J. A.; Bérces, A.; Bo, C.; Boerrigter, P. M.; Cavallo, L.; Chong, D. P.; Deng, L.; Dickson, R. M.; Ellis, D. E.; Fan, L.; Fischer, T. H.; Fonseca Guerra, C.; van Gisbergen, S. J. A.; Groeneveld, J. A.; Gritsenko, O. V.; Grüning, M.; Harris, F. E.; van den Hoek, P.; Jacobsen, H.; van Kessel, G.; Kootstra, F.; van Lenthe, E.; Osinga, V. P.; Patchkovskii, S.; Philipsen, P. H. T.; Post, D.; Pye, C. C.; Ravenek, W.; Ros, P.; Schipper, P. R. T.; Schreckenbach, G.; Snijders, J. G.; Sola, M.; Swart, M.; Swerhone, D.; te Velde, G.; Vernooijs, P.; Versluis, L.; Visser, O.; van Wezenbeek, E.; Wiesenekker, G.; Wolff, S. K.; Woo, T. K.; Ziegler, T. *ADF2002*; SCM, Theoretical Chemistry; Vrije Universiteit: Amsterdam, The Netherlands, 2002; http://www.scm.com.
(37) Fonseca Guerra, C.; Snijders, J. G.; te Velde, G.; Baerends, E. J. *Theor. Chem. Acc.* **1998**, *99*, 391.
(38) Velde, G. T.; Bickelhaupt, F. M.; Baerends, E. J.; Guerra, C. F.; van Gisbergen, S. J. A.; Snijders, J. G.; Ziegler, T. *J. Comput. Chem.* **2001**, *22*, 931.
(39) Parr, R. G.; Yang, W. *Density Functional Theory of Atoms and Molecules*; Oxford University Press: New York, 1989.
(40) Vosko, S. H.; Wilk, L.; Nusair, M. *Can. J. Phys.* **1980**, *58*, 1200.
(41) Becke, A. D. *Phys. Rev. A* **1988**, *38*, 3098.
(42) Lee, C.; Yang, W.; Parr, R. G. *Phys. Rev. B* **1988**, *37*, 785.
(43) Versluis, L.; Ziegler, T. J. *J. Chem. Phys.* **1988**, *88*, 322.
(44) Noodleman, L.; Norman, J. G., Jr. *J. Chem. Phys.* **1979**, *70*, 4903.

criteria (change in energy, 0.001 hartree; change in gradients, 0.01 hartree/Å; change in interatomic distances, 0.01 Å) were adopted, the gradient criterion used in the BS optimizations was substantially tighter (0.0001 hartree/Å), so as to accurately locate genuine minima upon the often rather flat potential energy surface.

Some comment is required on the methods used to infer bond orders, and related properties, from our computational results. In the trigonal symmetry of a face-shared complex $X_3MY_3M'Z_3$, the t_{2g} orbitals on each metal are split into the symmetry-distinct subsets a_1 (σ) and e (δ_π). The $S = 0$, $S = 2$, and $S = 3$ associated states for which valence d-electron occupancies are shown in Figure 1 provide a convenient framework through which to explore the properties of hypothetical complexes possessing, respectively, triple metal−metal bonds, single metal−metal bonds, and nonbonded (weakly coupled) metal atoms because the alignment or opposition of electron spin constrains the opportunities for bond formation through electron pairing. Note, also, that all of these associated states (including $S = 2$) are genuinely single-determinant configurations by virtue of the t_{2g} splitting imposed through the complex's trigonal symmetry. While only $S = 0$ corresponds precisely to a region on the antiferromagnetic $M_S = 0$ BS potential energy surface, the $S = 2$ and $S = 3$ associated states are essentially the ferromagnetic analogues of those regions on the BS surface in which the bond order is respectively one, or zero. For each associated state, the difference between the total number of valence electrons on each metal and the number of localized valence electrons corresponds to the metal−metal bond order. This correlation holds also for the BS-optimized minimum, for which the imposition of an initial spin asymmetry permits α-spin localization on one metal atom and β-spin localization on the other, in competition with the delocalization of M−M bond formation. Thus, the determination of the spin density on each metal, in the BS minimum, provides an essentially direct measure of the bond order.

As well as the above approach based on the Mulliken spin density on metal atoms, we have also employed the MAYER program[45] to determine Mayer bond orders, as defined elsewhere,[46] for the constituent bonds within the various BS optimized minima.

Results and Discussion

Our optimized geometries for the BS minimum and the minima of the various associated states of the $[X_3V(\mu\text{-}S(CH_3)_2)_3VX_3]^{2-}$ complexes are summarized in Table 1. Several aspects of the results of these calculations require comment. To begin with, it is desirable to assess our choice of the nonstandard VWN+B-LYP density functional as the optimal DFT method for exploring these potential energy surfaces. These are, after all, complexes for which the optimized metal−metal distance is extremely sensitive to the functional used, as is exemplified in Figure 2 by the potential energy curves for $[Cl_3V(\mu\text{-}S(CH_3)_2)_3VCl_3]^{2-}$ obtained using the VWN, VWN+B-LYP, and B-LYP functionals. The VWN result of $r(V-V) = 2.450$ Å (see Table 2) suggests an unambiguous triple bond between vanadium atoms, while the B-LYP value of $r(V-V) = 3.755$ Å is indicative of a complex featuring a weakly coupled antiferromagnetic interaction between V atoms. While the VWN+B-LYP $r(V-V)$ value of 2.592 Å is superficially similar to that obtained with VWN, the topography of the VWN+B-LYP potential energy surface differs as markedly from VWN as it does from B-LYP. The variation in the magnitude of the magnetic coupling is also evident in the values obtained for the calculated magnetic exchange constant[47] J using the different functionals. Which functional provides the most accurate picture of the V−V interaction in this complex, and in related structures?

We have attempted to answer this question, in a generic sense, through a recent survey of the DFT performance in the bond-length estimation for a diverse set of experimentally

Table 1. V−V Bond Lengths and Spin Densities for Optimized Geometries of $[X_3V^{II}(\mu\text{-}S(CH_3)_2)_3V^{II}X_3]^{2-}$ Complexes, Obtained Using the VWN+B-LYP Density Functional

formula	state	$r(V-V)$/Å[a]	E_{rel}/eV[b]	$\mu_{spin}(V)$[c]
$Cl_3V(\mu\text{-}S(CH_3)_2)_3VCl_3^{2-}$	BS	2.592	0	±1.07
	$S = 0$	2.505	0.009	0
	$S = 2$	3.093	0.677	1.96
	$S = 3$	3.689	0.273	3.02
	ref	3.661	2.750	0
$F_3V(\mu\text{-}S(CH_3)_2)_3VF_3^{2-}$	BS	2.694	0	±1.12
	$S = 0$	2.602	0.001	0
	$S = 2$	3.180	0.816	2.03
	$S = 3$	3.711	0.692	2.95
	ref	3.692	2.847	0
$(HO)_3V(\mu\text{-}S(CH_3)_2)_3V(OH)_3^{2-}$	BS	2.796	0	±0.002
	$S = 0$	2.770	0.006	0
	$S = 2$	3.392	0.970	1.94
	$S = 3$	3.891	0.746	2.87
	ref	3.840	2.732	0
$(H_2N)_3V(\mu\text{-}S(CH_3)_2)_3V(NH_2)_3^{2-}$	BS	2.967	0	0.000
	$S = 0$	2.959	0.001	0
	$S = 2$	3.558	1.085	2.06
	$S = 3$	4.043	0.733	3.23
	ref	3.969	2.462	0
$(HS)_3V(\mu\text{-}S(CH_3)_2)_3V(SH)_3^{2-}$	BS	2.584	0	±0.005
	$S = 0$	2.596	−0.003	0
	$S = 2$	3.091	0.885	1.84
	$S = 3$	3.735	0.605	2.97
	ref	3.728	2.807	0

[a] Optimized V−V separation for the indicated state. [b] Energy for the optimized structure for the indicated state, expressed relative to that found for the BS minimum. [c] Mulliken spin density on vanadium for the indicated state. These values have been "covalency-corrected" according to the procedure described in the text.

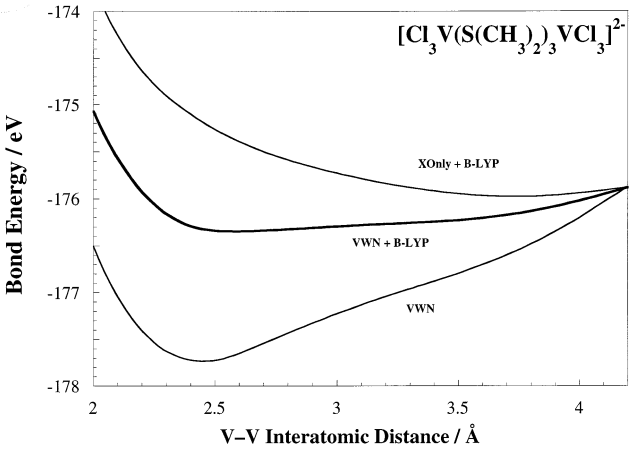

Figure 2. Potential energy curves, as a function of V−V internuclear separation, for the BS state of the $[Cl_3V(\mu\text{-}S(CH_3)_2)_3VCl_3]^{2-}$ complex, obtained using three different density functionals: VWN, VWN+B-LYP, and XOnly+B-LYP. To aid comparison of the potential energy curves, the VWN and XOnly+B-LYP values have been systematically shifted so that all three curves coincide at a V−V internuclear distance of 4.2 Å.

(45) Bridgeman, A. J.; Empson, C. *The MAYER program*; University of Hull: Hull, U.K., 2002. Freely available on the worldwide web from http://www.hull.ac.uk/php/chsajb/mayer/.
(46) Mayer, I. *Chem. Phys. Lett.* **1983**, *97*, 270.

Table 2. Comparison of Parameters Obtained for the BS Minima of $[X_3V(\mu\text{-}S(CH_3)_2)_3VX_3]^{2-}$ Complexes Obtained Using Different Functionals: VWN, VWN+B-LYP (Abbreviated Here as VB), and B-LYP

"terminal" ligand X	r(V−V)/Å			r(V−S)/Å[a]			μ_{spin}(V)[b]			$-J$/cm^{-1} [c]		
	VWN	VB	B-LYP	VWN	VB	B-LYP	VWN	VB	B-LYP	VWN	VB	B-LYP
Cl	2.450	2.592	3.755	2.273	2.444	2.675	0	1.07	3.14	996	245	47
F	2.570	2.694	3.391	2.267	2.371	2.575	0	1.12	2.78	1255	620	249
OH	2.689	2.796	3.773	2.288	2.363	2.658	0	0.002	2.2623	1337	668	293
NH_2	2.780	2.967	3.105	2.297	2.383	2.449	0	0	0		657	
SH	2.534	2.584	3.667	2.273	2.326	2.650	0	0.005	3.09	1268	542	98

[a] Optimized V−S (bridging sulfur) distance in the BS minimum. [b] Mulliken spin density on vanadium in the BS minimum. Values given include a covalency correction calculated from VWN+B-LYP calculations on the corresponding monomeric complex (see text for details). [c] Magnetic exchange constant, obtained as described in the text.

characterized dinuclear transition-metal complexes.[50] We found that VWN+B-LYP significantly outperformed all of the other methods surveyed, including standard VWN,[40] standard B-LYP,[41,42] Becke−Perdew (BP),[41,51] and Perdew−Wang91 (PW91),[52] for the estimation of metal−metal separations in dinuclear complexes, particularly complexes bearing a moderate overall charge (i.e., ±1 or ±2). Because the degree of metal−metal bonding is sensitively connected to the M−M distance, the further implication is that VWN+B-LYP is also the method of choice for determining the extent of valence d-electron delocalization, and therefore the bond order, within dinuclear complexes. One specific example from our survey[50] is particularly pertinent. The complex $[V_2(\mu\text{-}Cl)_3(thf)_6]^+$ is one[53−57] of only two[58] face-shared d^3d^3 complexes of vanadium to have been synthesized to date. It has been characterized by X-ray crystallography as possessing a V−V distance ranging from 2.97 to 3.02 Å.[54−57] For the model complex $[V_2(\mu\text{-}Cl)_3(O(CH_3)_2)_6]^+$, in which the tetrahydrofuran ligands have been replaced by dimethyl ether so as to reduce the duration of the calculations, we have obtained optimized values for r(V−V) of 2.814 Å using VWN and 3.121 Å with B-LYP, illustrating the respective tendencies of these methods to underestimate or to overestimate the metal−metal distance.[50] When VWN+B-LYP is used, we find r(V−V) = 2.980 Å, in excellent agreement with the crystallographic values. Note, also, that our methodological survey[50] showed that all methods exhibit weakened M−M bonding in complexes featuring a high overall absolute charge (for example, in "test set" calculations on trianionic and tetraanionic complexes); this is consistent with the distorting influence of Coulombic repulsion in "vacuum-phase" calculations on species which, in the crystalline state, are largely shielded against such distortion by the presence of neighboring counterions. In the present study, the dianionic complexes $[X_3V(\mu\text{-}S(CH_3)_2)_3VX_3]^{2-}$ are presumably subject to a moderate degree of such Coulombic distortion, which would be essentially absent in monocationic $[V_2(\mu\text{-}Cl)_3(O(CH_3)_2)_6]^+$. Thus, VWN+B-LYP is more likely to err toward a longer (weaker) V−V bond in $[X_3V(\mu\text{-}S(CH_3)_2)_3VX_3]^{2-}$ than would be found crystallographically.

Returning to Table 1, it is apparent that for each complex the various minima are consistently ranked in increasing total energy, with E(BS) ∼ $E(S=0)$ < $E(S=3)$ < $E(S=2)$ ≪ E(ref). The proximity of the BS minimum to the corresponding $S = 0$ minimum suggests that the V−V interaction is strong and approaches the nominal bond order of 3 expected for full metal−metal bonding in these species. However, our covalency-corrected[59] Mulliken spin densities for the vanadium atoms, μ_{spin}(V), show that the halide-terminated complexes still possess approximately one localized d-electron per V atom, implying a bond order of around 2 (see Table 2). The case for "full" V−V bonding appears more secure for those complexes in which the terminal ligands are OH^-, SH^-, or NH_2^-; here the calculated residual spin density on V, in the BS minimum, is negligible in each instance.

As an alternative evaluation of the reliability of the spin-density-based estimation of metal−metal bond orders described above, we have also determined bond orders accord-

(47) The constant J has been determined according to the convention $H = -2JS_1 \cdot S_2$, via the expression[48] $-2J = 2[E(S_{max}) - E_{BS}]/S_{max}^2$, for which S_{max} denotes the appropriate ferromagnetic state and for which the energies employed are those of the minima on the respective potential energy surfaces. In the present case, the two possible ferromagnetic states are $S = 2$ and $S = 3$; of these possibilities, $S_{max} = 3$ leads to substantially lower-magnitude J values than that which ensues on assignment of $S_{max} = 2$. We have previously[49] recommended that the more appropriate value of S_{max} is that which leads to the smaller J value; for the present family of V_2 complexes, this is consistently $S_{max} = 3$. Thus, for these dimers, J has been estimated using the relationship $J = -E_{rel}(S=3)/9$, where E_{rel} is the bond energy of the $S = 3$ minimum expressed relative to that for the BS minimum. Note, however, that this expression is strictly only valid for weakly antiferromagnetically coupled electrons and may therefore lead to considerable errors when strong coupling is present, as in the complexes investigated here. For this reason, these calculated J values should be regarded as indicative rather than precise.

(48) Noodleman, L. *J. Chem. Phys.* **1981**, *74*, 5737.
(49) Stranger, R.; Lovell, T.; McGrady, J. E. *Inorg. Chem.* **1999**, *38*, 5510.
(50) Petrie, S.; Stranger, R. *Inorg. Chem.* **2003**, submitted for publication.
(51) Perdew, J. P. *Phys. Rev. B* **1986**, *33*, 8822.
(52) Perdew, J. P.; Chevary, J. A.; Vosko, S. H.; Jackson, K. A.; Pederson, M. R.; Singh, D. J.; Fiolhais, C. *Phys. Rev. B* **1992**, *46*, 6671.
(53) Cotton, F. A.; Duraj, S. A.; Extine, M. W.; Lewis, G. E.; Roth, W. J.; Schmulbach, C. D.; Schwotzer, W. *J. Chem. Soc., Chem. Commun.* **1983**, 1377.
(54) Bouma, R. J.; Teuben, J. H.; Beukema, W. R.; Bansemer, R. L.; Huffman, J. C.; Caulton, K. G. *Inorg. Chem.* **1984**, *23*, 2715.
(55) Cotton, F. A.; Duraj, S. A.; Roth, W. J. *Inorg. Chem.* **1985**, *24*, 913.
(56) Cotton, F. A.; Duraj, S. A.; Manzer, L. E.; Roth, W. J. *J. Am. Chem. Soc.* **1985**, *107*, 3850.
(57) Canich, J. A. M.; Cotton, F. A.; Duraj, S. A.; Roth, W. J. *Polyhedron* **1987**, *6*, 1433.
(58) Gelmini, L.; Armstrong, W. H. *J. Chem. Soc., Chem. Commun.* **1989**, 1904.

(59) The raw Mulliken spin densities were corrected by a factor $3/\mu_{M(oct)}$, where $\mu_{M(oct)}$ is the Mulliken spin density obtained for the central vanadium atom within the isolated high-spin d^3 octahedral complex $X_3V(S(CH_3)_2)_3^-$ (X = Cl, F, OH, SH, or NH_2 as appropriate). The purpose of this correction factor is to allow for the effect of metal−ligand covalency within the octahedral complex and, by analogy, also in the corresponding dinuclear complex: covalency reduces the spin density from the value of 3 expected for a purely ionic complex of V^{II}.

Table 3. Determination of Metal−Metal Bond Orders for the BS Minima of $[X_3V(\mu\text{-}S(CH_3)_2)_3VX_3]^{2-}$ Complexes, via Mulliken Spin-Density and Mayer Bond-Order Analyses

"terminal" ligand X	*r*(V−V)/Å[a]	μ_{spin}(V)[b] raw[c]	corr.[d]	BO[e]	Mayer BO.[f] BO_{BS}[g]	$BO_{S=0}$[g]	BO_{corr}[h]
Cl	2.592	0.963	1.07	1.93	1.635	1.896	2.59
F	2.694	0.937	1.12	1.88	1.473	1.751	2.52
OH	2.796	0.0002	0.0002	3.00	1.362	1.471	2.78
NH_2	2.967	0	0	3.00	1.110	1.122	2.97
SH	2.584	0.0004	0.0005	3.00	1.668	1.660	3.01

[a] Optimized V−V distance in the BS minimum. [b] Analysis based on Mulliken spin density on vanadium in the BS minimum. [c] Uncorrected value of the vanadium Mulliken spin density, obtained directly from the VWN+B-LYP BS geometry optimization. [d] Covalency-corrected Mulliken spin density, using the covalency correction factor obtained from VWN+B-LYP calculations on the corresponding monomeric complex (see text for details). [e] Spin-density-derived bond order, obtained by subtracting the covalency-corrected μ_{spin}(V) value from the hypothetical maximum V−V bond order of 3 (see text for details). [f] Analysis using the MAYER program[45] to determine Mayer bond orders. [g] Mayer bond order for the V−V bond, for the identified (BS or $S = 0$) optimized geometry. [h] "Corrected Mayer" bond order, obtained by multiplying the ratio BO_{BS}:$BO_{S=0}$ by the hypothetical maximum V−V bond order of 3 (see text for details).

ing to the Mayer approach[46] as implemented in the program MAYER.[45] The results obtained from this analysis are detailed in Table 3. The Mayer analysis supports our spin-density-based technique insofar as both methods invariably determine V−V bond orders of greater than unity for the sulfur-bridged dinuclear complexes. However, it is apparent from Table 3 that the V−V Mayer bond orders obtained for the BS-optimized geometries of the various complexes are consistently and significantly lower than those gleaned from the spin-density approach. There is also a monotonic trend toward decreasing V−V Mayer bond order with increasing intermetallic separation in the BS minimum, which is not reflected in the spin-density-derived values. We believe that the best reconciliation between these two measures of bond order can be achieved by determining also the Mayer bond orders for the corresponding $S = 0$ optimized geometries, in which the delocalization of all metal-based electrons between the two metal centers effectively dictates a V−V bond order of 3 (i.e., one σ and two δ_π covalent V−V bonds) in each instance. These $S = 0$ Mayer bond orders, which like the BS values are all between 1 and 2, clearly indicate the considerable influence of metal−ligand bond covalency on the calculated metal−metal bond order. A crude correction for covalency can be implemented through the expression $BO_{corr} = BO_{max}BO_{BS}/BO_{S=0}$, where BO_{max} is the hypothetical maximum (d^3d^3) V−V bond order of 3. When this correction is applied, the "covalency-corrected Mayer bond orders" (see Table 3) give a trend that conforms qualitatively to that seen with the corrected Mulliken spin-density approach. One striking result is that both the Mulliken and Mayer approaches ultimately yield metal−metal bond orders for all of these complexes of at least 1.8, much higher than those apparent for any face-shared, first-transition-row complexes to have been studied previously.

The factors influencing the interactions between V atoms, in the Cl-terminated complex, are further explored in Figures 3−5. The electronic configuration for the BS minimum, shown in Figure 3, substantiates the inference already drawn

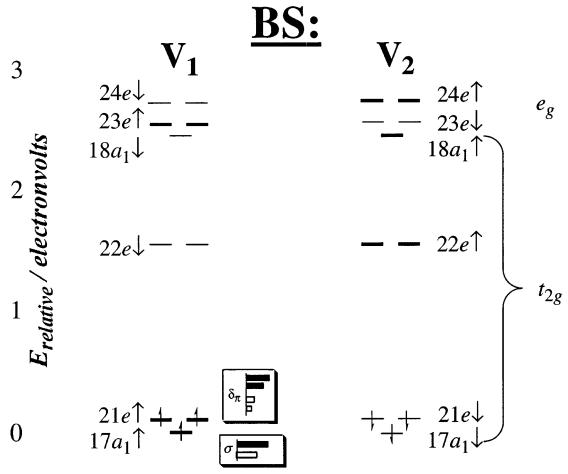

Figure 3. Electronic configuration of the BS minimum of the $[Cl_3V(\mu\text{-}S(CH_3)_2)_3VCl_3]^{2-}$ complex (obtained using the VWN+B-LYP combination of functionals), showing the valence-d metal-dominated orbitals. Metal AO contributions to the occupied α-spin MOs are displayed as overlaid bar charts, with V_1 and V_2 AOs shown as filled (black) and outlined (white) bars, respectively. For the occupied α-spin $17a_1$ (σ) orbital, the V_1 and V_2 AOs which contribute to the MO character are d_{z^2}; for 21e, the two AOs depicted for each vanadium atom are respectively $d_{x^2-y^2}$ (or d_{xy}) and d_{xz} (or d_{yz}). Contributions to the corresponding occupied β-spin MOs have the V_1 and V_2 character transposed in each instance.

from structural and spin-density data concerning the degree of metal−metal bonding in this complex. The occupied a_1-symmetry valence-d metal-based molecular orbital (MO) is largely delocalized between the two metal atoms V_1 and V_2, with the slight residual spin asymmetry in the resulting σ bond being reflected in the disparity (~59:41%) between the contributions of the two metal atoms to the α-spin MO. A substantially greater spin asymmetry is exhibited in the occupied e-symmetry orbitals, with 76% of the α-spin metal-based character derived from V_1 atomic orbitals (AOs). Both of the bonding 21e and antibonding 22e orbital manifolds can be categorized as δ_π orbitals, and therefore identified as t_{2g}-based MOs, because they conform to the expectation that (for example) the $d_{x^2-y^2}$ contribution is approximately double that of d_{xz}. In contrast, the 23e and 24e manifolds display π_δ character (e.g., with d_{xz} dominant over $d_{x^2-y^2}$). Disproportionation of the MO character, between V_1 and V_2, is almost identical in antibonding $18a_1$ to that shown for the bonding orbital $17a_1$, and a similar correspondence in V_1 and V_2 contributions is evident also for 21e and antibonding 22e. While significant delocalization between the metal atoms is thus apparent in all of these t_{2g}-based MOs, the e_g-based MOs are almost completely localized either on V_1 or V_2 and (understandably) display a much greater degree of "contamination" from ligand S and Cl AOs than from AOs on the other metal atom. Finally, it should also be stated that the MO analysis depicted in Figure 3 shows that the major factor in the strong antiferromagnetic coupling between V_1 and V_2 is indeed the direct interaction between metal atoms and not superexchange involving the bridging sulfur atoms. This provides an important distinction between these thioether-bridged complexes and the oxo-bridged Cr(III) and Mn(IV) complexes,[23,60] for which substantial antiferromagnetic coupling (and short metal−metal separations) have been

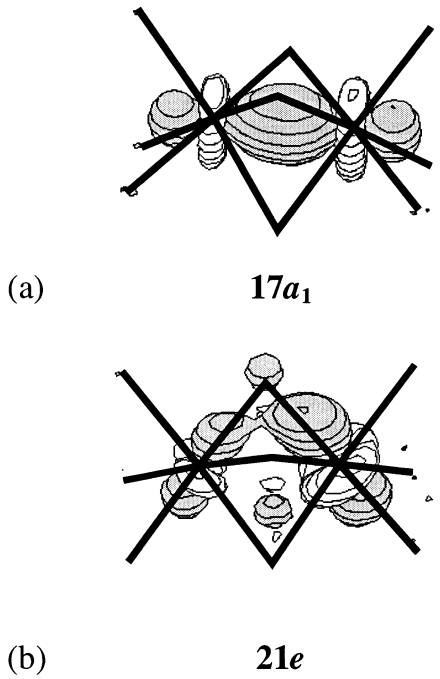

Figure 4. Depiction of the β-spin, valence metal-based orbitals for the $[Cl_3V(\mu\text{-}S(CH_3)_2)_3VCl_3]^{2-}$ complex, at a contour level of 0.060 in each instance. Bonds between Cl, V, and S aroms are overlaid in bold. These orbital diagrams show that most of the V_1/V_2 spin asymmetry in the BS minimum for this complex derives from the δ_π-bonding 21e orbital manifold rather than the σ-bonding $17a_1$ MO. (Note that the significant ligand-based orbital character in the 12e manifold, apparent in Figure 4b, is centered on the thioethers' methyl groups, for which atomic positions have not been shown in these diagrams.)

experimentally determined and shown to arise mainly from superexchange via the oxo bridges.[16] Figure 4 provides a further graphic demonstration of the overwhelming importance of direct metal−metal bonding, rather than superexchange, as the conduit for the strong coupling exhibited in (for example) the chloride-terminated complex. In this figure the contribution arising from S- and Cl-based orbitals, to the character of the metal-based valence orbitals, is seen to be essentially insignificant.

Figure 5 displays the BS potential energy curve for the Cl-terminated complex as a function of the V−V distance, with curves also shown for the $S = 0$, $S = 2$, and $S = 3$ associated states in the vicinity of their respective minima. At short V−V separations, the BS curve follows that for the "triply bonded" $S = 0$ associated state, and at substantially larger V−V distances, the BS and $S = 3$ curves are seen to converge, but it is notable that the BS curve always lies substantially below the (nominally σ-bonded) $S = 2$ curve. This mismatch between BS and $S = 2$ energies arises because of the imposition of D_{3h} symmetry on the electronic configuration in the $S = 2$ complex, ensuring that the σ-symmetry MOs of this complex are fully delocalized between the two vanadium atoms. The constraint of a full σ bond between V_1 and V_2 in the $S = 2$ associated state is rather unfavorable: recall above that, at a V−V distance only

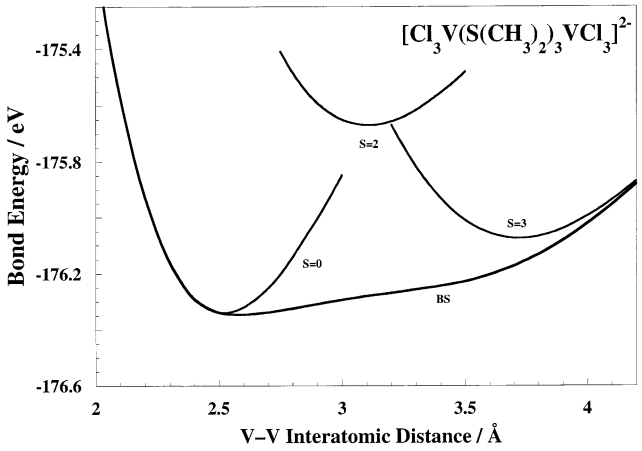

Figure 5. Potential energy curve, as a function of V−V internuclear separation, for the BS state of the $[Cl_3V(\mu\text{-}S(CH_3)_2)_3VCl_3]^{2-}$ complex, obtained using the VWN+B-LYP combination of functionals. Also shown are the curves due to the $S = 0$, $S = 2$, and $S = 3$ associated states, in the vicinities of their respective minima.

0.1 Å greater than that of the triply bonded $S = 0$ minimum, the BS minimum already features an 18% excess of V_1 content over V_2 in the analogous α-spin $17a_1$ orbital. Because the $S = 2$ minimum features a rather larger V−V distance than that seen for BS, the drive toward localization of the valence electrons on one or another metal atom is considerable but is frustrated by the formalism of the $S = 2$ calculation, which artificially enforces σ-bond formation in a less than ideal geometric configuration.

The "energy gap" between the $S = 2$ minimum and the BS state at the same V−V distance is considerably larger than the corresponding mismatch between $S = 2$ and BS energy values for other multiply bonded, face-shared dimers, such as $Mo_2Cl_9^{3-}$, which we have studied.[13,50] It is instructive to examine the unpaired (and uncorrected) Mulliken spin density on each metal atom, in the BS structure with the M−M separation at the $S = 2$ optimum value. For the chloride-terminated V^{II} dimer, $\mu_{spin}(BS) = 2.22$ at the $S = 2$ V−V separation of 3.09 Å. Using the $S = 2$ and $S = 3$ μ_{spin} values of 1.76 and 2.71 to describe bond orders of 1 and 0, respectively, the BS μ_{spin} value corresponds to a V−V bond order of only 0.52; thus, the $S = 2$ associated state minimum possesses an enforced doubling of the V−V bond order preferred at this separation. In contrast, the "typical" second-transition-row dimer $Mo_2Cl_9^{3-}$ exhibits $\mu_{spin}(BS) = 2.02$ at the $S = 2$ optimum Mo−Mo separation, corresponding to a bond order of 0.73 (when assessed against the $S = 2$ and $S = 3$ uncorrected spin densities for $Mo_2Cl_9^{3-}$). Obviously, the $S = 2$ enforcement of bond order 1 represents a less severe distortion of the preferred bond order at that Mo−Mo separation in this second-row dimer, and we speculate that the exaggerated $E(S{=}2) - E(BS)$ gulf for the V^{II} dimers may relate to a difference in properties of the valence d orbitals between the first-row and the heavier transition metals. Note that because the structures described here are the first known examples of first-row, face-shared dimers possessing multiple metal−metal bonding, it is perhaps unsurprising that this apparently distinguishing characteristic of first-row complexes has evaded identification until now.

(60) Wieghardt, K.; Bossek, U.; Nuber, B.; Weiss, J.; Bonvoisin, J.; Corbella, M.; Vitols, S. E.; Girerd, J. J. *J. Am. Chem. Soc.* **1988**, *110*, 7398.

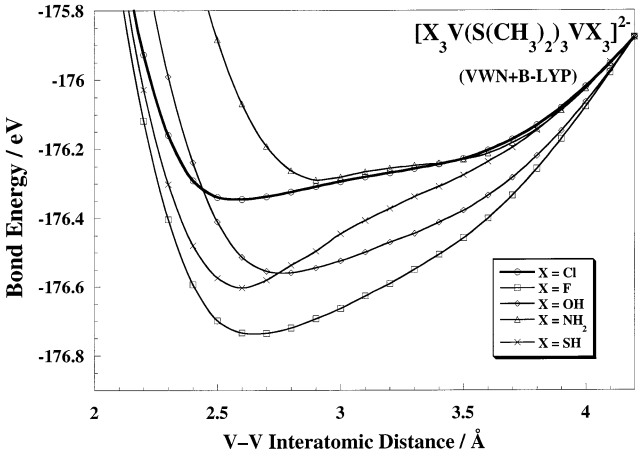

Figure 6. Potential energy curves, as a function of V−V internuclear separation, for the BS state of the $[X_3V(\mu\text{-}S(CH_3)_2)_3VX_3]^{2-}$ complex, obtained using the VWN+B-LYP combination of functionals, for different terminal ligands X: Cl^-, F^-, OH^-, SH^-, and NH_2^-. To aid comparison of the potential energy curves, the values for X = F^-, OH^-, SH^-, and NH_2^- have been systematically shifted so that all curves coincide at a V−V internuclear distance of 4.2 Å.

Figure 6 provides a comparison of BS potential energy curves for the various $[X_3V(\mu\text{-}S(CH_3)_2)_3VX_3]^{2-}$ complexes. All of these curves feature a characteristically broad potential well, for which the minimum is located toward the short end of the V−V distance scale, with a comparatively gentle increase in slope until r(V−V) approaches 4 Å. This figure demonstrates, in agreement with the data given in Table 1, that these complexes consistently feature multiple metal−metal bonds according to the VWN+B-LYP combination of functionals. Nevertheless, perusal of the energy scale also indicates that the energetic requirement for substantial lengthening of the V−V separation, and concomitant localization of the valence-d metal-based electrons, is not severe in any of these instances. In this regard, the sulfur-bridged face-shared V_2 complexes may provide an interesting example of "metal bond plasticity", analogous to the $Mo_2X_9^{3-}$ (X = Cl, Br, I) complexes for which considerable variation in the metal−metal distance is evident in crystallographic studies.[8,61−63]

As characterized by μ_{spin}(V) in Table 1, there is not a tidy correlation between the apparent V−V bond order and the V−V distance in the BS minima for the various $[X_3V(\mu\text{-}S(CH_3)_2)_3VX_3]^{2-}$ complexes. Indeed, the "double" bond in the Cl-terminated complex is almost identical in length to the "triple" bond of the HS-terminated species and much shorter than the V−V distances found for the other triply bonded complexes (i.e., those terminated by OH^- and by NH_2^-). Why should this be so, when the same bridging ligands are common to all complexes? Comparison of values listed in Tables 1 and 4 shows that there is a reasonable correlation between increasing V−V distance in the BS minimum and decreasing unpaired (monomeric) spin density μ_{spin}(V), and a similar correlation of the BS V−V separation

Table 4. Spin Polarization Stabilization Energies E_{SPE} and, Where Applicable, d-Orbital Overlap Energies E_{ovlp} for "Monomeric" $[((CH_3)_2S)_3VX_3]^-$ and "Dimeric" $[X_3V^{II}(\mu\text{-}S(CH_3)_2)_3V^{II}X_3]^{2-}$ Complexes (X = Cl, F, OH, SH, NH_2)[a]

"terminal" ligand X	$[((CH_3)_2S)_3VX_3]^-$		$[X_3V(\mu\text{-}S(CH_3)_2)_3VX_3]^{2-}$		
	μ_{spin}(V)[b]	$2E_{SPE}$/eV[c]	E_{SPE}/eV[c]	E_{ovlp}/eV[d]	$E_{SPE} - E_{ovlp}$/eV[c,d]
Cl	2.694	2.230	2.477	2.741	−0.264
F	2.501	2.046	2.155	2.846	−0.691
OH	2.458	1.940	1.986	2.726	−0.740
NH_2	2.098[e]	1.450[e]	1.729	2.461	−0.732
SH	2.637	2.074	2.202	2.810	−0.608

[a] All values shown here were obtained from VWN+B-LYP calculations. [b] Uncorrected Mulliken spin density on the vanadium atom. [c] E_{SPE} is the "spin polarization stabilization energy", E(ref state) − $E(S_{max})$. [d] E_{ovlp} is the "d-orbital overlap energy", E(ref state) − $E(S{=}0)$. [e] The complex $[((CH_3)_2S)_3V(NH_2)_3]^-$ is unstable against concerted loss of the dimethyl sulfide ligands. Values reported are for a partially optimized structure having r(V−S) fixed at 2.50 Å, which is the mean V−S distance found from the BS and various associated state minima.

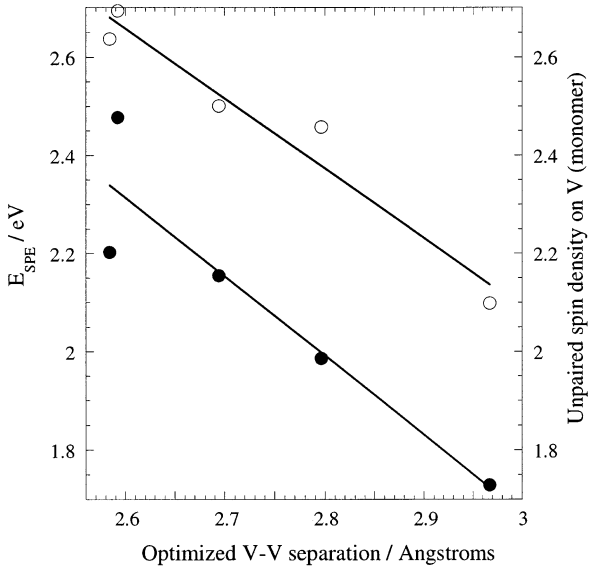

Figure 7. Graph showing the correlation between the BS-optimized V−V distance and two parameters associated with the spin state of the vanadium atoms. The data indicate values for the (dimeric) spin polarization stabilization energy E_{SPE} (filled circles), in electronvolts, and the (monomeric) unpaired Mulliken spin density on vanadium (empty circles).

with E_{SPE} (in the dimer) is also evident (see Figure 7). No such consistent trend is seen for V−V distance versus E_{ovlp}. The correlation between metal atom spacing and the unpaired-spin parameters shown in Figure 7 shows that a reduction in the magnitude of the effective spin density on the metal atoms accompanies the elongation of the V−V triple bond in the complexes with OH^- and NH_2^- terminal ligands. We attribute this "spin dampening" to the substantial covalency of the V−X bonds when the terminal ligands X are NH_2 or OH. It appears that the driving force for triple bond formation with these terminal ligands is the tendency for these ligands to quench the spin polarization stabilization of ferromagnetic (or weak antiferromagnetic) coupling in a weakly coupled complex: thus, it is not any heightened bond strength of the triply bonded configuration itself but rather the relative instability of the main structural alternative that enforces the multiple metal−metal bonding in these complexes. The bond lengthening in the NH_2- and OH-terminated

(61) Subbotin, M. Y.; Kazin, P. E.; Aslanov, L. A.; Zelentsov, V. V. *Koord. Khim.* **1985**, *11*, 1568.
(62) Subbotin, M. Y.; Aslanov, L. A. *Zh. Neorg. Khim.* **1986**, *31*, 393.
(63) Stranger, R.; Smith, P. W.; Grey, I. E. *Inorg. Chem.* **1989**, *28*, 1271.

complexes would appear to result from increasing valence d-orbital dilation on V with increasing V−X bond covalency. The net result is the counterintuitive finding that the triple V−V bonds in the OH^-- and NH_2^--terminated complexes are appreciably longer than the nominal "double" bonds in the halide-terminated complexes.

The question remains, can these complexes be synthesized? We would argue that the isolation and crystallographic characterization of the heavier congeners $[X_3M(\mu\text{-tht})_3MX_3]^{2-}$ (M = Nb, X = Cl, Br; M = Ta, X = Cl; tht = tetrahydrothiofuran),[33] which show very strong structural similarity to the Cl-terminated vanadium dimer considered here, is a very promising indicator that the V-containing species may also be synthetically attainable. The second- and third-row $[X_3M(\mu\text{-tht})_3MX_3]^{2-}$ dimers, which invariably feature robust M−M triple bonds, are reported to be both air- and water-stable.[33] In a previous study,[22] we have reported the results of DFT calculations on the analogous $[Cl_3M(\mu\text{-}S(CH_3)_2)_3MCl_3]^{2-}$ complexes for which calculated M−M distances are found to be very close to those seen crystallographically.[33] On a methodological note, the slight overestimation of Nb−Nb and Ta−Ta separations by our VWN calculations in the earlier work,[22] compared to the crystallographic values,[33] is contrary to the general tendency of VWN to underestimate intermetallic separations. Because the VWN+B-LYP method always[50] yields longer M−M values than those gleaned by VWN, it would also appear that VWN+B-LYP should overestimate, rather than underestimate, the V−V distances in the complexes of interest in this work.

Concluding Remarks

Our DFT calculations using the VWN+B-LYP combination of functionals have shown that the series of $[X_3V(\mu\text{-}S(CH_3)_2)_3VX_3]^{2-}$ complexes investigated here all possess significant metal−metal bonding, with calculated bond orders of 2−3 in all cases. Analysis of Mulliken spin densities, of Mayer bond orders, and of the metal-based valence MOs supports the inference that the substantial antiferromagnetic stabilization ($-J > 250\ cm^{-1}$) observed in these complexes derives from the direct interaction between metal atoms rather than through superexchange involving the bridging S atoms. The $[X_3V(\mu\text{-}S(CH_3)_2)_3VX_3]^{2-}$ complexes are thus apparently the first examples of mutiply bonded, face-shared first-transition-row dinuclear complexes to have been investigated. While experimental evidence to support this assertion is as yet lacking, we note that very close Nb(II)- and Ta(II)-containing structural analogues of these complexes have been isolated, are air- and water-stable, and also possess multiple metal−metal bonds.

Acknowledgment. We gratefully acknowledge the Australian Research Council (ARC) for financial support. We also thank Dr. German Cavigliasso for his assistance with the Mayer bond order calculations.

IC026276K